

Magnetic coupling across a ferromagnetic-metal–alkali-metal interface

J. S. Payson, R. E. Brauer, and G. L. Dunifer

Department of Physics and Astronomy, Wayne State University, Detroit, Michigan 48202

(Received 8 September 1995)

We report on an experimental study of the interfacial magnetic coupling in metallic bilayers consisting of an alkali metal and a thin ferromagnetic film. The alkali metals used were either potassium or lithium, with the ferromagnetic metal consisting of either iron or Permalloy. This study began as part of a larger project consisting of a study of Larmor waves in potassium. Our observations will also be of interest to those studying magnetic multilayers, in which the nature of the magnetic coupling between ferromagnetic and nonmagnetic metals plays an important role. In this paper, we show how the degree of magnetic coupling in these bilayer samples can be examined by studying the interaction of the ferromagnetic resonance of the ferromagnetic film with the conduction-electron spin resonance (CESR) of the alkali-metal layer. These studies are carried out at cryogenic temperatures (down to 1.1 K) using microwave reflection spectroscopy at 12 GHz. We have also examined the temperature dependence of the magnetic resonances. Between 1.1 and 25 K, for both lithium and potassium, an unexpected *narrowing* of the CESR lines occurs with increasing temperature.

I. INTRODUCTION

This article reports the results of an experimental investigation of the magnetic coupling between a paramagnetic alkali metal (potassium or lithium), and a ferromagnetic metal (iron or Permalloy). The nature of interfacial magnetic coupling is currently of considerable interest as indicated by the large number of investigations underway of magnetic multilayers and their properties. This study grew out of a larger project consisting of a detailed study of Larmor waves¹ in alkali metals at liquid-helium temperatures.

Larmor waves are microwave transmission signals carried across thin plates of pure metal in the presence of a dc magnetic field by ballistic electrons, which are able to travel from one surface of the sample to the other without scattering. The signal results from the free Larmor precession of the electron spins during the transit time across the sample. As compared to spin waves, which are a collective-wave phenomenon involving all the electrons on the Fermi surface, Larmor waves are actually single-particle excitations and involve electrons on small portions of the Fermi surface for which the phase of the spin precession has some extremal property. Because of the small number of electrons involved, Larmor waves are generally too weak to be observed unless special techniques are used to enhance the amplitude of the signal.

The enhancement technique has generally consisted of applying thin ferromagnetic layers to the surfaces of the sample. It was noted by Janossy and Monod² that the coupling between an incident microwave field and the spin of a conduction electron in a metal could be strongly enhanced by the application of a thin ferromagnetic film. By applying such ferromagnetic layers to both surfaces of a sample, it is possible to enhance the Larmor-wave spectra by a factor of several hundred to a few thousand,¹ thus enabling their detection. Using this technique, Larmor waves were discovered in copper and gold by Janossy and Monod³ in 1976. For the original observation, the ferromagnetic layers consisted of a few hundred angstroms of either evaporated Permalloy or an amorphous alloy of cobalt and phosphorus.⁴ In a more thor-

ough investigation of the coupling mechanism between the ferromagnetic and paramagnetic metals, Silsbee, Janossy, and Monod⁵ studied, by microwave transmission, the conduction-electron spin resonance (CESR) of copper foils onto which thin films of Permalloy, iron, or nickel had been evaporated. For the analysis of their data, they developed a phenomenological theory from the appropriate Bloch equations for the magnetization of the copper and ferromagnetic films. The two media were coupled by the transport of magnetization across the interface by diffusion of electrons. The theory quite well described a number of features in the experimental data and indicated that the coupling process takes place predominantly through the following steps: (1) within the ferromagnet the microwave magnetic field couples to the large magnetization of the localized *d* electrons, (2) the *s* electrons in the ferromagnet are driven by the *d* electrons through an exchange interaction, and (3) the itinerant *s* electrons diffuse across the interface carrying transverse magnetization into the copper.

Relatively little has been published on the experimental observations of Larmor waves in metals. The early studies were done on either copper,^{1,3,5} gold,^{1,3} or tungsten¹ at X-band frequencies (~ 9 GHz). More recently, we published⁶ a report on the study of Larmor waves in single-crystal copper at a frequency of 80 GHz. In contrast to the earlier observations at 9 GHz, the higher-frequency study found a Larmor-wave period, which was temperature dependent and, at the lowest temperatures for certain orientations, an asymmetry in amplitude with respect to the CESR signal. This behavior was not in complete agreement with the Larmor-wave theory of Montgomery and Walker,⁷ and it was suggested that it might be because of a combination of many-body effects and the detailed geometry of the Fermi surface of copper. In an effort to find a metal whose Larmor-wave signal would be easier to interpret, we initially selected potassium. The conventional picture⁸ of potassium is that of a metal with a spherically symmetric Fermi surface, having an exchange interaction among the conduction electrons that has been well characterized by a detailed study of its spin-

wave spectrum.⁹ Potassium is generally considered to have the simplest electronic structure of all metals and to be closest to many of the models used by theorists in their calculations of various metallic properties.

In order to study the Larmor-wave spectra of potassium, it was first necessary to develop a method for applying thin ferromagnetic layers, which have good magnetic coupling to the conduction electrons of the potassium. This is considerably more difficult than for copper. The chemically reactive potassium easily acquires an oxide layer, which can prevent any magnetic coupling from taking place. After trying several different techniques, suitable magnetic coupling was achieved by depositing potassium and the ferromagnetic material in rapid succession inside of a high-vacuum system. Later, bilayers containing lithium were produced in a similar manner in order to compare their characteristics with those of the potassium bilayers. For the ferromagnetic film, we have selected either iron or Permalloy (an alloy of mostly nickel and iron). In the study of Silsbee, Janossy, and Monod,⁵ Permalloy generally gave stronger CESR signals in transmission and considerably narrower ferromagnetic-resonance (FMR) linewidths than either iron or nickel separately. On the other hand, when a broader FMR line was useful, e.g., in our transmission studies, we found that iron works well. The properties of these bilayer samples are described in the remainder of this article.

II. EXPERIMENTAL TECHNIQUE

A small stainless-steel UHV chamber was constructed in which the alkali metal was deposited by evaporation and the ferromagnetic film was deposited by either evaporation or sputtering. The ferromagnetic metal was first deposited onto a glass or quartz substrate followed, in quick succession, by the alkali-metal evaporation directly on top of the ferromagnetic metal. In this report, results were obtained using either Permalloy films deposited by dc sputtering or iron films, which were thermally evaporated. This necessitates a vacuum system capable of combining the sputtering and evaporation processes in rapid succession. The internal dimensions of the chamber are 8 in. in diameter \times 8 in. in length. These dimensions were chosen so that (1) the small volume could be quickly pumped from sputtering conditions (10^{-1} Torr) to evaporation conditions ($<10^{-4}$ Torr), and (2) the chamber can be removed from the pumping system and taken through an airlock into a dry box. To minimize oxidation of the alkali metals, a dry box is used to first load the alkali metals into an evaporation boat prior to making the sample, and then, once again, in the assembly of the sample after the depositions have taken place. Two gate valves connected to the chamber allow it to be transported under vacuum between the pumping system and the dry box. This assures the worst environment that the sample is exposed to is that of the dry box.

A Vacuum/Atmospheres dry-box system containing argon gas is used. The atmosphere is continually circulated through three different traps (including a hot titanium sponge at 900 °C), which remove water vapor, oxygen, and nitrogen and keep their concentration <1 ppm. A freshly exposed potassium surface in the box will last at least 6 h before any tarnish can be seen with the naked eye; lithium remains un-

tarnished for many days. During the sputtering process, ultrahigh-purity argon gas from the dry box is used.

In order to achieve good magnetic coupling between the alkali metals and the ferromagnetic film, it is necessary to have a clean, nonoxidized interface. This requires the transition from the deposition of the ferromagnetic layer to the alkali-metal deposition be short compared to the monolayer formation time,¹⁰ τ_m :

$$\tau_m = 4/(n\xi^2v_{av}) \approx 1.86 \times 10^{-6}/P, \quad (1)$$

where n is the number density of the gas, ξ is the molecular diameter, and v_{av} is the average molecular velocity. In the second form of the equation, evaluated for air at room temperature, P is the partial pressure in Torr of the reactive component of the atmosphere, and τ_m is given in seconds. The base pressure of the system is 10^{-8} Torr. At either the base pressure or during sputtering at 10^{-1} Torr with 99.9999 at. % ultrahigh-purity argon gas, τ_m is at least tens of seconds. On the other hand, during the evaporation of the alkali metal or iron, the pressure rises to $\approx 10^{-6}$ Torr, making τ_m of the order of several seconds, depending on what percentage of the residual gas can react with the deposited metals. This suggests that the change from the ferromagnetic-metal to the alkali-metal deposition should be made within about 1 s or less. This is easily done when both metals are evaporated, by simply rotating the substrate from one deposition region to the other, which is accomplished in a fraction of a second. To satisfy this requirement in the case of the sputter deposition of Permalloy, we have selected a turbomolecular pump with a pumping speed of 150 ℓ/s . According to standard calculations of pumping rates,¹⁰ our combination of the turbomolecular pump with large-diameter vacuum plumbing enables the chamber pressure to be reduced from 10^{-1} to 10^{-4} Torr in 1.3 s.

In the construction of the UHV chamber and pumping system, copper gaskets and Conflat flanges are used everywhere with the exception of a single viton O ring between the chamber and its cover. The ungreased viton O ring allows for quick assembly and disassembly of the chamber within the dry box. The glass substrate is mounted on a water-cooled heat sink that can be rotated so that the substrate can be positioned directly above either the Permalloy sputtering-target-iron-evaporation source or the alkali-metal evaporator. A stainless-steel or tantalum mask determines the geometry of the deposited material. The alkali-metal evaporator consists of a 0.005-in. thick tungsten or molybdenum boat, heated by an ac current. A thermocouple, spot welded to the boat, is used to monitor its temperature. For deposition of Permalloy, simple dc sputtering is used instead of the more complicated magnetron or rf sputtering. Typical sputtering conditions consisted of a pressure of 110 mTorr of ultrahigh-purity argon gas, an applied voltage of 3000 V, a sputtering current of 7 mA, with the substrate placed 2.6 cm above the Permalloy target. The iron evaporator consists of a thin plate of iron suspended a few mm above a pair of thoriated-tungsten filaments. The emitted electron beam, accelerated through a potential of ~ 700 V, impacts the iron plate from below, heating it to the evaporation temperature (slightly below the melting temperature).

The following sequence of steps was worked out, which consistently produced samples having good magnetic cou-

pling between the ferromagnetic material and the alkali metal.

- (1) The sample chamber is baked out at 100 °C for 24 h. After cooling to room temperature, the pressure in the chamber drops to about 7×10^{-8} Torr.
- (2) The chamber is removed from the pumping system and transported under vacuum to the dry box, where the alkali metal is transferred from a storage ampoule to the evaporation boat.
- (3) The chamber is reattached to the pumping system, pumped, and baked out at 100 °C for an additional 24 h. After cooling to room temperature, the chamber pressure is $2\text{--}3 \times 10^{-8}$ Torr.
- (4) Cooling water is supplied to the substrate heat sink. When sputtering is used, presputtering of the target is carried out for 20 min to condition the target by removing any oxide layer present on the surface.
- (5) The substrate is then rotated above the sputtering unit or iron evaporator to begin the deposition of Permalloy or iron. Both the Permalloy and iron were deposited at a rate of 0.3–0.5 Å/s to give a total thickness of 200–400 Å in about 12 min.
- (6) During the deposition of the ferromagnetic material, the temperature of the alkali-metal evaporation boat is slowly ramped above the melting temperature of the alkali metal. During the last 3 min of the deposition of the ferromagnetic material, the temperature is brought up to the evaporation temperature of the alkali metal. These temperatures are approximately 250 °C and 320 °C for the potassium and lithium, respectively.
- (7) Within a 1-s period the following operations are carried out: (a) the substrate is rotated over the alkali-metal evaporator and (b) when sputtering, the flow of argon gas into the chamber is terminated and the gate valve to the pumping system is fully opened, dropping the chamber pressure to $<10^{-4}$ Torr.
- (8) The alkali metals are evaporated at a rate of 0.1–0.2 $\mu\text{m/s}$ to give a total thickness of about 10–200 μm .
- (9) The chamber is allowed to cool for 1 h. It is then taken again into the dry box under vacuum, where the chamber is opened, the sample is removed, coated with a thin layer of vacuum grease, and placed into a microwave cavity for studying the FMR of the ferromagnetic layer and the CESR of the alkali metal.

The thicknesses of the deposited films were determined in a variety of ways. For the ferromagnetic layer, the film was deposited separately on a glass substrate, and three different techniques were used at different times: (a) an analysis of Rutherford back-scattering spectra, (b) a mechanical thickness measurement with a diamond-stylus profilometer, and (c) optical transmission measurements through the partially transparent films. For the alkali metal, a micrometer was used to measure the thickness of the deposited material me-

chanically on the mask surrounding the sample itself. For two potassium samples, an even more accurate thickness determination was made by recording the cyclotron-wave¹¹ transmission spectra at the same time as the FMR and CESR measurements were ongoing.

The magnetic-resonance data are taken using standard techniques. The microwave reflection spectrometer operates at a frequency of 12 GHz and employs magnetic-field modulation with phase-sensitive detection so that the detected signal is proportional to the field derivative of the absorbed power. The sample can be surrounded by a liquid-helium bath and the temperature varied from 1.1 K to room temperature. The dc magnetic field, provided by a 12-in. Varian electromagnet, has a range of 0–13 kG and can be rotated in the horizontal plane through an angle of 360°. The sample is mounted in a TE₁₀₁ rectangular cavity on a vertical side wall so that the dc magnetic field can be rotated relative to the plane of the sample.

This geometry allows one to vary the resonance field of the FMR by changing the demagnetizing field¹² and thereby determine the effective magnetization $4\pi M$ of that film. The resonance fields H_0^\perp and H_0^\parallel , for orientations perpendicular or parallel to the plane of the specimen, respectively, are given by

$$\omega/\gamma = H_0^\perp - 4\pi M \quad (2)$$

and

$$(\omega/\gamma)^2 = H_0^\parallel(H_0^\parallel + 4\pi M), \quad (3)$$

where γ is the gyromagnetic ratio of the magnetic moments. For the perpendicular orientation, the resonance field is shifted higher than the usual value of $H_0 = \omega/\gamma$ by the dc demagnetizing field, $4\pi M$. For the parallel orientation, the resonance field is shifted lower than ω/γ by an ac demagnetizing field. A measurement of the resonance fields for the two orientations allows a determination from Eqs. (2) and (3) of both $4\pi M$ and γ of the ferromagnetic film.

III. OBSERVATIONS

A. Potassium bilayers

High-purity potassium metal obtained from Callery Chemical Co. was used in the experiment. The potassium was stored in glass ampoules under argon gas, and the ampoules used have been in our possession for about 17 yr. We tried using potassium purchased within the past 2 or 3 yr but discovered that the newer material displayed no CESR or spin-wave resonances that could be detected by either reflection or transmission microwave spectroscopy. The newer material is presumably contaminated in some way, but we made no additional efforts to determine the nature of the contaminant. The potassium that we used had bulk residual resistance ratios $\rho(295 \text{ K})/\rho(1.1 \text{ K})$ of 3000–8000 and residual CESR linewidths as narrow as 0.2 G in our best material at 1.1 K. Potassium evaporated directly on top of glass or quartz substrates had a typical residual linewidth of 2 G, still reasonably narrow for CESR studies and also narrower than that observed when the potassium was deposited directly on top of a ferromagnetic film.

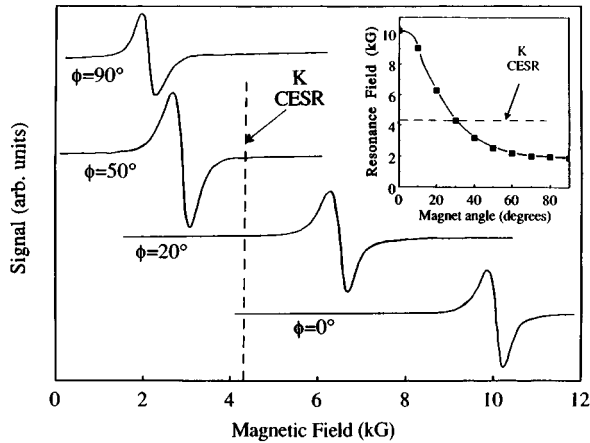


FIG. 1. Typical FMR data in Permalloy showing the effects of the demagnetizing field for four different orientations of the applied field. Inset: The resonance field vs the magnet-orientation angle ϕ .

FMR measurements made on bulk material from the Permalloy sputtering target gave a value for $4\pi M$ of 7.2 kG at room temperature and 8.0 kG at 77 K. For calibration purposes, the Permalloy was first sputtered onto glass substrates without a potassium overlayer. Typical thicknesses used in the initial studies, as well as in the later bilayer samples, were in the range of 200–400 Å, which is less than the microwave skin depth. The films were checked visually for uniformity and transparency. A typical value of $4\pi M \approx 6$ kG obtained for our Permalloy thin films, corresponds to a magnetization of about 70% of that of the bulk starting material in the target. An analysis of thin films of iron of similar thicknesses also reveal the same behavior, i.e., the effective magnetizations are also about 70% of the bulk value of 21.5 kG.

Figure 1 shows typical FMR data for a Permalloy film as the applied magnetic field is rotated from the parallel to the perpendicular orientation. The angle ϕ is measured between the applied field and the direction normal to the plane of the sample. The center of the FMR line can be varied over a range of about 8 kG because of the changing demagnetizing fields associated with different field orientations. The inset in the figure displays the complete angular dependence of the resonance field. The peak-to-peak linewidth is approximately 500 G and nearly independent of the angle ϕ . For bilayer samples containing Permalloy, the FMR linewidths vary between 200 and 450 G and are usually at least a factor of 20 times broader than the CESR linewidths observed in the potassium overlayers. The dashed lines in the figure indicate the position of the fixed potassium CESR signal (4.28 kG), as determined by its g value⁹ of 2.000 07. As can be seen, the FMR resonance field of the Permalloy can be swept through the position of the potassium CESR by rotating the applied field. The two resonances coincide at a critical angle, which has a typical value $\phi_{\text{crit}} \approx 30^\circ$. For a single potassium layer, the CESR amplitude is independent of ϕ . On the other hand, in a bilayer sample, if the spins of the conduction electrons in the potassium are driven primarily by the magnetization of the Permalloy, then the CESR amplitude should display a considerable enhancement around the angle ϕ_{crit} . This is how we have monitored the degree of magnetic coupling in the bilayer samples.

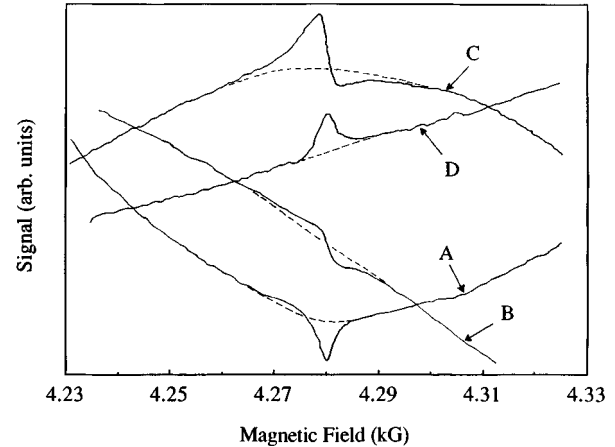


FIG. 2. Typical traces from a Permalloy-potassium sample with moderate magnetic coupling showing the potassium CESR signal superimposed on top of the Permalloy FMR. (a) $\phi = 31.5^\circ$; relative gain=4. (b) $\phi = \phi_{\text{crit}} = 30.0^\circ$; relative gain=1. (c) $\phi = 29.0^\circ$; relative gain=4. (d) $\phi = 25.0^\circ$; relative gain=10.

In contrast to the Permalloy films, the linewidth of iron depends quite strongly on the direction of the applied magnetic field. The linewidth starts out at about 200–300 G for the applied field parallel to the surface of the sample and increases generally by a factor of 2 or 3 as the direction of the applied magnetic field approaches the normal to the plane of the sample. We were unable to track the behavior of the iron FMR all the way to the perpendicular geometry, since the maximum value of the applied magnetic field was insufficient to overcome the large internal demagnetizing fields of the thin film. The two resonances (FMR of iron and the CESR of potassium) coincide at a critical angle, which has a typical value $\phi_{\text{crit}} \approx 16^\circ$.

We have made and studied approximately 25 Permalloy-potassium samples (15 studied via reflection and 10 by transmission) and 10 iron-potassium samples (three studied via reflection and seven by transmission). The reflection studies are reported here; the transmission studies will be reported separately.¹³ The degree of magnetic coupling between the ferromagnetic film and the potassium remained fairly strong and constant from sample to sample when evaporated iron was employed; considerable variation from sample to sample occurred when sputtered Permalloy was used. In general, an increased magnetic coupling resulted in both an enhanced CESR signal strength and an increased broadening of the CESR linewidth. The strongest CESR lines usually displayed the maximum linewidths.

In Fig. 2 we display for a Permalloy-potassium specimen a series of 100-G field sweeps, centered on the potassium CESR, for four different values of ϕ near ϕ_{crit} . This sample has moderate magnetic coupling with a relatively strong, but narrow, CESR line, which is easily seen for all angles near ϕ_{crit} . The CESR is situated on a varying baseline, which is a portion of the Permalloy FMR, whose overall amplitude is about 20 times larger than that of the CESR. The CESR linewidth is 4.0 G, while that of the FMR is 260 G. The dashed-line segments are a smooth continuation of the FMR baseline in the vicinity of the CESR signal. Two features of the CESR are evident in Fig. 2: (a) the variation of ampli-

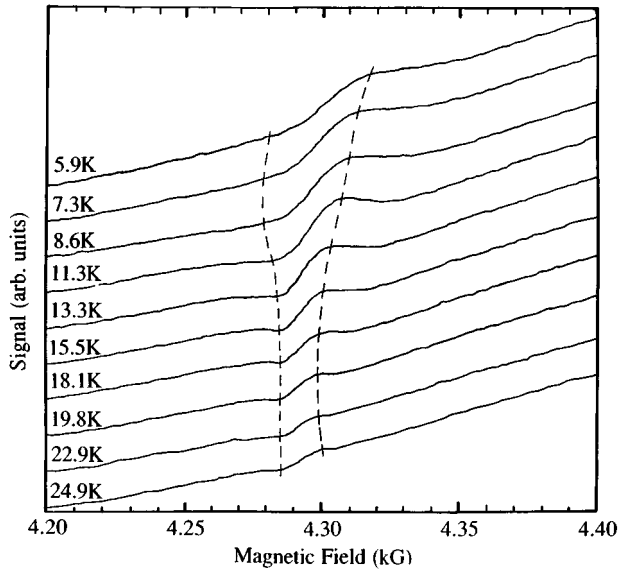


FIG. 3. Potassium CESR spectra taken from a Permalloy-potassium sample having very strong magnetic coupling. The angle ϕ is held constant at 22° for a range of different temperatures. The FMR linewidth is approximately 350 G. The dashed lines indicate the narrowing of the CESR linewidth with temperature.

tude with angle ϕ (note the different gains used for the separate traces) and (b) the variation in phase of the signal with ϕ . Plotted as a function of the angle ϕ , the CESR amplitude shows a relatively sharp, nearly symmetric peak centered at ϕ_{crit} . This is one clear indication that the CESR within the potassium is being driven primarily by the magnetism of the thin ferromagnetic film rather than the microwave fields directly. And, as discussed in detail in Sec. IV, the variation in phase of the CESR signal with respect to the angle ϕ provides further evidence that the Permalloy layer provides the dominant driving mechanism of the conduction electrons in the potassium.

We have also examined the temperature dependence of the resonance signals over the range 1.1–25 K. The Permalloy FMR remains essentially constant over this limited temperature range, whereas in a single potassium layer the CESR is strongly temperature dependent, rapidly broadening at higher temperatures because of an increased spin-flip scattering rate induced by thermal phonons. For a Permalloy-potassium bilayer, it is observed that the CESR enhancement is strongly temperature dependent and rapidly *decreases* at higher temperature. As an example of the temperature dependence, we show in Fig. 3 a series of potassium CESR lines in a bilayer sample for a fixed value of ϕ . Each trace is taken at a constant temperature, which ranges from 5.9 to 24.9 K. For the selected value $\phi=22^\circ$, the CESR is superimposed on the tail of the FMR, which is centered at a higher magnetic field to the right of the figure. This magnetic-field orientation gives sufficient enhancement so that the CESR is visible at each temperature but also a baseline, which varies sufficiently slowly that the CESR is not obscured. It is clear from the figure that the amplitude of the signal decreases at higher temperature. An indication of the linewidth, taken as the distance between the positive and negative lobes in this derivative spectrum, is indicated by the dashed curves in the figure.

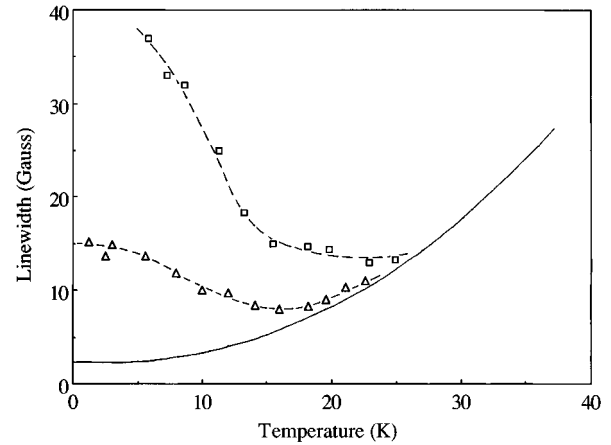


FIG. 4. Temperature dependence of the potassium CESR linewidth for three samples. Solid line: single potassium plate without a ferromagnetic surface layer. Square symbols: Permalloy-potassium sample with very strong magnetic coupling plotted for $\phi=22^\circ$. The FMR linewidth is 350 G. Triangular symbols: Permalloy-potassium sample with weaker magnetic coupling plotted for $\phi=34^\circ$. The FMR linewidth is 230 G. The dashed lines in the figure serve only as a guide for the eye.

As can be seen, the CESR linewidth actually *decreases* with increasing temperature, in opposition to what occurs in a single potassium layer. The narrowing between the lowest and highest temperatures in Fig. 3 is almost a factor of 3.

For another perspective on the influence of temperature, Fig. 4 shows the temperature dependence of the CESR linewidth for three different samples. The solid curve is for a single potassium plate without a ferromagnetic surface layer, whose CESR was monitored via transmission spectroscopy with the field oriented parallel to the sample's surface. The residual linewidth of 2.2 G, seen at the lowest temperatures, is caused by spin scattering from impurities in the sample. The contribution to the linewidth from phonon scattering becomes evident for temperatures above 5 K. The difference between the full curve plotted in Fig. 4 and the residual linewidth, gives the phonon contribution alone (as would be seen in an ideal sample without impurities). This is the minimum linewidth possible for any sample at a given temperature.

The other two samples in Fig. 4 are potassium-Permalloy bilayers, which were observed by reflection spectroscopy with the applied magnetic field oriented close to ϕ_{crit} . Once again, both of these samples show linewidths that *decrease* with increasing temperature above 5 K. The sample indicated with the triangular symbols has a residual linewidth of 15.2 G and a minimum linewidth of 8 G at 16 K. For higher temperatures, the linewidth again broadens as the contribution from phonon scattering begins to play a role. The other sample, indicated by the square symbols, has stronger magnetic coupling and also displays a considerably broader CESR line. The line is so broad at the lowest temperatures that it is undetectable; it becomes observable only after it begins to narrow at the higher temperatures. For this sample, the signal-to-noise ratio is sufficiently poor by the temperature where phonon broadening begins, that a linewidth minimum is not clearly visible.

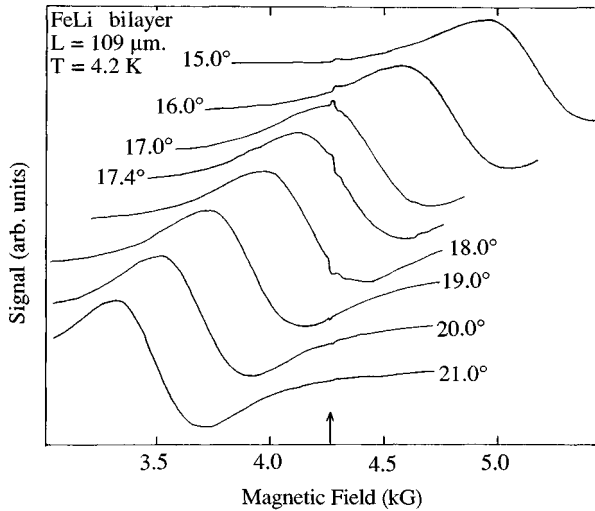


FIG. 5. Typical resonance data from an Fe-Li bilayer. The temperature and gain are held constant for a series of traces taken with different magnetic-field orientations. Each trace is labeled with the angle ϕ . The arrow shows the location of the fixed Li CESR signal.

Samples made with iron instead of Permalloy show exactly similar trends. The major differences are different demagnetizing fields, critical angles, and FMR linewidths. Some of these differences are particularly useful for the microwave transmission studies, to be reported.¹³ Another advantage of iron is that the iron-potassium bilayers showed strong interfacial coupling more consistently from sample to sample.

B. Lithium bilayers

Lithium is an ideal choice for further study of the phenomena described above, since it has a narrow, temperature-independent CESR linewidth, in contrast to the linewidth of pure potassium, which increases monotonically with temperature. This characteristic of lithium results from a very weak spin-orbit coupling, which does not couple the conduction-electron spins to thermal phonons to any significant extent. This allows us to investigate the CESR linewidth in lithium bilayers over the whole temperature range 1.1–300 K without the complications of phonon-induced spin-flip scattering. We have studied only bilayers of iron and lithium, and what we observe is exactly analogous to the properties of Permalloy-potassium or iron-potassium bilayers, except that the signals are generally larger and more easily monitored. A total of 11 samples were observed (nine by reflection and two by transmission).

The interaction of the FMR and CESR for an Fe-Li bilayer sample can be directly seen in Fig. 5, for several different magnet angles. Clearly seen is the increasing resonant field of the FMR as the magnetic field direction approaches the normal of the sample. The lithium CESR is superimposed on the FMR line at a fixed field. As the two lines cross, the CESR phase changes and the amplitude increases. When the two lines are exactly superimposed the CESR reaches a maximum intensity. Beyond this point the phase continues changing, while the amplitude of the CESR signal decays. A careful analysis of this type of data shows that the total shift

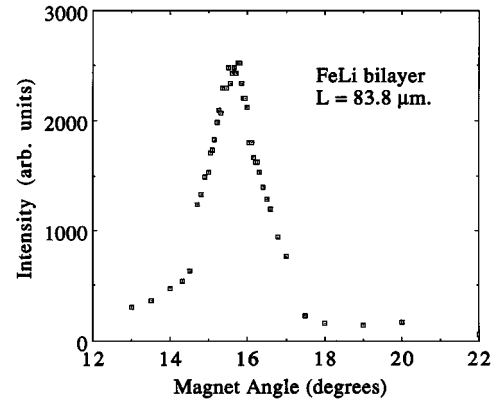


FIG. 6. The lithium CESR intensity as a function of the angle ϕ for an Fe-Li sample at a temperature of 4.2 K.

in phase of the CESR is about 360° as the FMR moves from one side of the CESR to the other.

In Fig. 6 we have plotted the “intensity” of the CESR as a function of the angle ϕ for an Fe-Li bilayer of thickness $83.8 \mu\text{m}$. The data were recorded at a temperature of 4.2 K. For intensity we use a quantity that is proportional to the area under the χ'' (power-absorption) curve, a quantity that, for a single layer, is proportional to the magnetic susceptibility of the sample and independent of the spin-relaxation rate. Our magnetic-resonance spectrometer uses magnetic-field modulation, with $H_{\text{mod}} \ll \Delta H_{\text{CESR}} \ll \Delta H_{\text{FMR}}$, where ΔH_{CESR} and ΔH_{FMR} are the linewidths of the CESR and FMR, respectively. Under these conditions the peak amplitude of the CESR signal is given by

$$\text{peak amplitude} = \frac{C \times \text{intensity} \times H_{\text{mod}}}{\Delta H_{\text{CESR}}^2}, \quad (4)$$

where C is a constant. Equation (4) is used to obtain a properly normalized intensity for plotting in Fig. 6 and also Fig. 8 below. It also provides a method for comparing different samples with each other on a quantitative basis. In the calculation of the intensity for Fig. 6 an allowance was also made for the variation of signal phase with the angle ϕ . As can be seen from the figure, the intensity of the CESR is a strong function of ϕ , showing a sharp, nearly symmetric peak centered at ϕ_{crit} . The overall width of the peak is a function of ΔH_{FMR} and the rate at which the FMR resonance field changes with ϕ in the vicinity of ϕ_{crit} .

Using data from the same sample above, the strong temperature dependence of the CESR intensity is shown in Fig. 7. Here the intensity is shown at a fixed magnet angle $\phi = 15.6^\circ$ as the temperature is varied. We observe that for $T < 10$ K there is little change in the intensity, but as the temperature increases beyond 10 K we see a dramatic decrease. Between 20 and 40 K the decrease follows an approximate power law of T^{-4} .

Additional data from the same sample is displayed in Fig. 8, where the CESR linewidth is given as a function of the temperature. The linewidth increases from about 2 G at 70 K to about 37 G at 10 K. At the lower temperatures the amount of broadening is related to the thickness of the alkali-metal layer, with thinner samples having larger linewidths. The residual low-temperature linewidth appears to be inversely

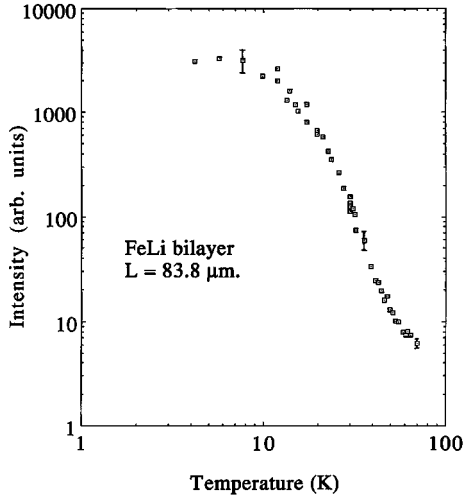


FIG. 7. Temperature dependence of the lithium CESR intensity at $\phi=15.6^\circ$ for the same sample plotted in Fig. 6.

proportional to the specimen thickness. In all cases, as the temperature increases, the linewidth decreases toward the linewidth of a single layer of lithium. We have also made several samples with iron on both sides of the lithium and find that the linewidth is about twice as broad as one would find for the same thickness of a bilayer. Two of these samples were assembled by pressing two bilayer samples together inside the dry box to form a sandwich structure. The clean alkali-metal surfaces immediately bond to each other, forming a single lithium layer with iron on both outside surfaces. An added advantage of this method is that during the pressing, some lithium was squeezed out from the region where the iron was deposited. This excess lithium was not magnetically coupled to the iron and provided a very convenient g marker. We have observed that the g value of the CESR line was independent of both the temperature and the magnet angle ϕ . This is generally true for all bilayer samples independent of whether they contain lithium or potassium.

A final observation is displayed in Fig. 9, which shows the modulation of the FMR and CESR linewidths as a function

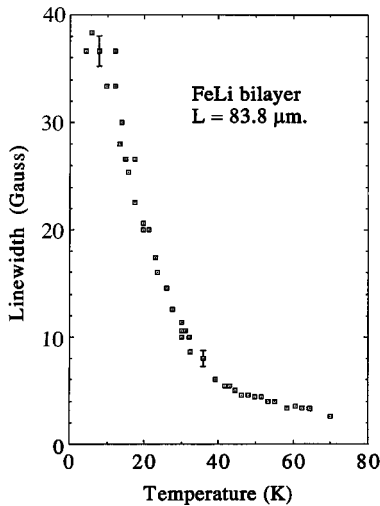


FIG. 8. Temperature dependence of the lithium CESR linewidth at $\phi=15.6^\circ$ for the same sample plotted in Fig. 6.

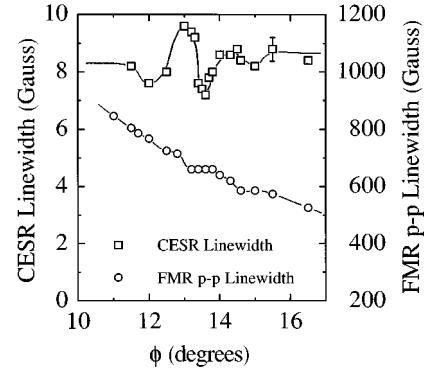


FIG. 9. Modulation of the FMR and CESR linewidths in the vicinity of ϕ_{crit} for an Fe-Li specimen 3.48×10^{-2} cm thick measured at a temperature of 4.2 K. The solid lines serve only as a guide for the eye. The experimental error for the FMR linewidth is smaller than the size of the symbols used.

of the angle ϕ as the FMR is swept through the CESR near ϕ_{crit} . This modulation is a result of the coupling that occurs between the two resonances. The two linewidths oscillate up and down approximately out of phase with each other, i.e., as one is passing through a maximum, the other is passing through (or near) a minimum. Similar behavior occurs with all of the other types of bilayer samples we have studied. We have been very careful to assure ourselves that the modulation of the FMR linewidth is *not* an artifact caused by the simple superposition of the two resonance lines on top of each other. The modulation is relatively small on the FMR, being typically 3–6%. On the CESR the modulation is more, typically 15–25%. In calculating the angular dependence of the CESR intensity in Fig. 6, we have used the average CESR linewidth in Eq. (4) in order not to introduce complicating fine structure into the figure. The theory of Silsbee, Janossy, and Monod⁵ neglects the back reaction of the s electrons on the d electrons in the ferromagnetic film. As seen from the FMR linewidth near ϕ_{crit} , this is not strictly valid, but in view of the relatively small modulation of the FMR line, it appears to be a reasonably good approximation.

IV. DISCUSSION

We have given a description of our sample-fabrication technique and shown how the degree of magnetic coupling in this class of samples can be monitored by studying the interaction between the FMR and CESR signals. We have gone into considerable detail in Sec. II, as it is important that all nine steps of the sample-fabrication procedure outlined there be carried out in order to achieve a high degree of magnetic coupling. Relaxation of any of the steps in this procedure results in reduced magnetic coupling within the final sample.

We have not attempted to make a detailed comparison of our experimental data with the theory of Silsbee, Janossy, and Monod⁵ because those theoretical calculations have been derived for microwave transmission measurements, whereas our observations have been carried out using reflection spectroscopy. The two techniques generate signals having both different amplitudes and line shapes. Furthermore, transmis-

sion measurements have a distinct advantage in that the FMR and CESR signals can be totally separated from each other (in the absence of accidental microwave leakage around the sample). This makes it possible to carry out very precise measurements of the CESR line shape and its phase. On the other hand, with reflection measurements the FMR and CESR are necessarily superimposed on each other. The FMR always dominates in amplitude and linewidth, providing a variable baseline on which the CESR is situated. For certain ranges of the angle ϕ , especially for the broader CESR lines, the exact baseline becomes somewhat ambiguous, leading to considerable uncertainties in both the CESR line shape and its phase.

It is possible, however, to compare a few features of the theory with the experimental data. The theory was derived under a number of simplifying assumptions: (1) the applied field is normal to the surface of the sample, (2) its magnitude is $>4\pi M$, (3) the skin depth in the paramagnetic metal is classical, (4) there is no direct spin relaxation at the interface, and (5) the thickness of the paramagnetic metal is less than the spin-diffusion distance (or spin depth) δ_s . The spin depth δ_s corresponds to the rms-average distance a conduction electron diffuses in a spin lifetime. Not all of the conditions above are necessarily satisfied in our samples; nevertheless, the model calculation includes the effects of most of the physical processes going on within a bilayer sample and allows us to look for a few expected features within the data.

One of the most prominent characteristics of our data, clearly seen in Figs. 2 and 5, is the change of phase of the CESR signal as the magnetic field direction is rotated through the angle ϕ_{crit} . This phase change is proof that the conduction electrons are being driven primarily by the magnetization of the ferromagnetic film rather than the microwave fields directly. According to both the theory and experimental data on Permalloy-Cu of Silsbee, Janossy, and Monod [see, for example, Fig. 3(a) of Ref. 5], the CESR phase changes by 180° as the center of the FMR is swept from the low-field to the high-field side of the CESR. The reason for this follows. As is well known for a resonant system, the phase of the response of the system with respect to the driving force changes continuously as one sweeps through the resonance. When the frequency of the driving force $\omega \ll \omega_0$, i.e., the natural frequency of the system, the system responds in phase to the driving force (but with a small amplitude). When $\omega = \omega_0$ at resonance, the response of the system lags the driving force by 90° in phase (achieving its maximum amplitude), and, when $\omega \gg \omega_0$, the system lags by 180° in phase (again with a small amplitude). In this same way, the phase of the precessing ferromagnetic spins, with respect to the driving microwave fields, changes by 180° as one sweeps from the high-field tail of the FMR line, through the center of the resonance, out to the low-field tail of that line. Because $\Delta H_{\text{CESR}} \ll \Delta H_{\text{FMR}}$, when the two resonances are in close proximity (ϕ is near ϕ_{crit}), only a small fraction of the FMR line is sampled while sweeping through the complete CESR resonance. Over this limited field range, the phase of the ferromagnetic spins remains essentially constant relative to the microwave fields. However, this phase can be varied through 180° , depending on which portion of the FMR line is superimposed on top of the CESR. In this manner, the phase of the CESR signal observed by Silsbee, Janossy, and

Monod⁵ changes by 180° as the complete FMR line is swept past the fixed CESR line by a rotation of the applied magnetic field.

As noted earlier, however, in our data we observe a total change of approximately 360° in the CESR signal as the FMR line is swept through it. This difference is because of the different ways in which the data are obtained for the two experiments. For the transmission measurements of Silsbee Janossy, and Monod on copper,⁵ the microwave fields are incident on the side consisting of the ferromagnetic layer. Then, as described earlier, the microwaves drive the ferromagnetic layer, which, in turn, drives the spins of the conduction electrons of the copper. The detected copper CESR signal is then radiated from the uncoated surface into the free space on the opposite side of the sample. In this way, the ferromagnetic layer is used once, at one surface of the specimen, to couple the input power to the itinerant spins. For our reflection measurement, the ferromagnetic layer is effectively used twice: first, to couple the microwave power to the itinerant spins, and second, to enhance the detection of the induced CESR moment. This is equivalent to what would occur in transmission for ferromagnetic layers deposited on both surfaces of a specimen. Since for reflection the FMR enhancement is used twice, one would expect that the enhancement factor appropriate for transmission should be squared, resulting in a phase shift of 360° over the tuning range of the FMR, rather than 180° . Indeed, careful measurements of the CESR phase, out onto the extreme wings of the FMR, where both signals are very weak, show an overall variation close to 360° .

Another prediction of the theory of Silsbee, Janossy, and Monod⁵ can be obtained from Eq. (28) in Ref. 5, which gives for the linewidth of the CESR signal

$$\Delta H = \frac{2}{\gamma_p} \left[\frac{1}{T_2} + \frac{\Gamma'}{\chi_p L} \right], \quad (5)$$

where the parameters describing the conduction electrons of the paramagnetic component (potassium or lithium) of the bilayer sample are γ_p , the gyromagnetic ratio; T_2 , the bulk spin-spin relaxation time; and χ_p , the Pauli paramagnetic susceptibility. The quantity L is the thickness of the alkali-metal layer, and Γ' is a phenomenological parameter describing the rate of transport of transverse magnetization across the interface between the two metals. (The parameter Γ' takes into account the back reaction of the s electrons in the alkali metal on the s electrons in the ferromagnet.) The first term on the right-hand-side of Eq. (5) represents the contribution to the CESR linewidth from bulk scattering events such as from impurities and thermal phonons. The second term represents an additional linewidth broadening caused by the interfacial magnetic coupling. According to the equation this additional broadening should be inversely proportional to the thickness of the paramagnetic layer. In Fig. 10 we show a plot for several lithium bilayers of the CESR linewidth minus the bulk linewidth (0.6 G) versus $1/L$, the reciprocal of the thickness. The linewidths plotted are the residual, low-temperature linewidths of each sample. Also plotted in this figure are two trilayer samples having ferromagnetic layers on both surfaces. As can be seen from the

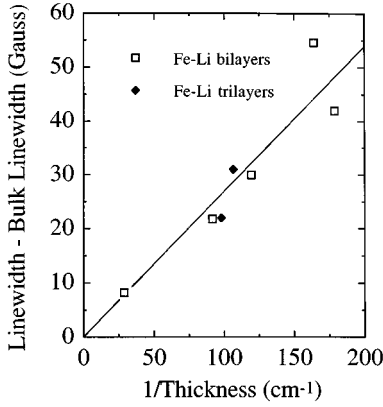


FIG. 10. The residual lithium CESR linewidth minus the bulk linewidth vs the reciprocal of the thickness of the lithium layer. Square symbols: Fe-Li bilayers with the full linewidth plotted. Diamond symbols: Fe-Li trilayers (sandwich samples) with half the linewidth plotted. Straight line: least-squares linear fit to the bilayer data.

figure, the data do fit quite well to a linear relationship. The straight line represents a least-squares linear fit to the data from the bilayer samples. The scatter from the linear relation can be readily interpreted as caused by (1) variations of the parameter Γ' among the individual samples, i.e., variations in the degree of interfacial magnetic coupling because each individual sample is fabricated under slightly different conditions, (2) uncertainties in identifying the exact baseline for each CESR trace, and (3) uncertainties in the thickness determination. The theory was derived assuming that the alkali-metal thickness $L \ll \delta_s$, a condition that is satisfied for the samples plotted in Fig. 10 (see Table I below). Under this condition the conduction electrons are able to diffuse back and forth several times across the sample within a spin lifetime via a random-walk process. Accordingly, a given electron is thus equally likely to be found anywhere within the volume of the sample, including the ferromagnetic layer. As the thickness of the paramagnetic layer is reduced, the total time the electron spends in contact with the ferromagnetic layer should thus increase as $1/L$. The effective coupling between the localized d electrons and itinerant s electrons will then increase as $1/L$ as well. This is reflected in Eq. (28) of Ref. 5 in both the $1/L$ dependence of the transmission-signal amplitude as well as the $1/L$ dependence in the line-broadening term [Eq. (5) above]. For the trilayer samples, the linewidth is essentially doubled from what would be seen for a bilayer sample of the same thickness. For this reason we have plotted $(\Delta H - \Delta H_{\text{bulk}})/2$ for the two trilayer samples on Fig. 10, and, as can be seen, they also lie reasonably close to the straight line on the figure. Presumably, when $L \ll \delta_s$ and ferromagnetic layers are present on both surfaces, the conduction electrons of the alkali metal will encounter the interfaces at twice the bilayer rate, thereby doubling the coupling of these electrons to the d electrons at the surfaces.

To the extent that we can neglect interfacial relaxation of the spins, Eq. (5) can be used to estimate the magnetization-transport parameter Γ' from the CESR linewidth. The Pauli susceptibility of the alkali metal χ_p is needed for the calculation, and this is listed in Table I for potassium and lithium. Also listed in the table for these metals are typical values of

TABLE I. Typical parameters at $T=1.1$ K for the potassium and lithium used for this study.

Parameters	Potassium	Lithium
Effective mass ratio m^*/m_0	1.21 ^a	2.20 ^b
Fermi velocity v_F (10^7 cm/s)	7.1	5.9
Pauli susceptibility χ_p (10^{-6} cgs volume units)	0.91 ^c	2.3 ^d
Residual resistance ratio	5000	700
Scattering time τ (10^{-11} s)	23	1.2
Mean free path Λ (10^{-3} cm)	17	0.77
CESR linewidth ΔH (G)	2.0	0.60
Spin lifetime T_2 (10^{-8} s)	5.7	19
Spin depth δ_s (10^{-2} cm)	21	7.2

^aReference 30.

^bReference 31.

^cReference 9.

^dReference 23.

several other parameters, which will be used later in the discussion. We have calculated Γ' for two Permalloy-K samples with moderate to strong coupling. For these samples we have taken $2/\gamma_p T_2 = 2.2$ G (the linewidth observed in a single layer of evaporated potassium). We have also calculated the average value of Γ' for five Fe-Li samples by using the slope of the linear fit to the data in Fig. 10. The calculated values of Γ' are listed in Table II. The first entry in the table corresponds to the Permalloy-K sample having the strongest coupling that we produced. For that sample the CESR linewidth at 1.1 K was so broad that it could not be accurately measured. For this reason, the calculation was carried out at 5.9 K, where the linewidth (and apparent coupling strength) are less.

From the parameter Γ' we can estimate the interfacial transmission coefficient t for the conduction electrons at the boundary between the two metals. Calculations of the coefficient t have been considered by Menard and Walker¹⁴ as well as by Silsbee, Janossy, and Monod.⁵ Making the assumption that $\Gamma' \approx \Gamma$, where the parameter Γ neglects the back reaction of the s electrons in the paramagnetic metal on the s electrons in the ferromagnetic metal, Silsbee, Janossy, and Monod⁵ obtain their Eq. (46):

$$\Gamma' \approx \Gamma = \frac{v_F \chi_p t}{4} \frac{1}{1 - \frac{1}{2}(t_p + t_f)}, \quad (6)$$

where v_F is the Fermi velocity, and t_p and t_f are the transmission coefficients for the conduction electrons approaching the interface from the side of the paramagnetic metal or the ferromagnetic metal, respectively. The product $(v_F \chi_p t)$ in Eq. (6) is the same for either metal, as can be shown by detailed balance arguments. Making the same assumption as Silsbee, Janossy, and Monod⁵ that $t_p = t_f = t$ and using the values of v_F listed in Table I, we obtain, for t , the quantities listed in the last column of Table II. As can be seen, there is not a large variation in the values of Γ' or t between the Permalloy-K and the Fe-Li specimens. For comparison purposes, we have also listed the parameters obtained by Silsbee, Janossy, and Monod⁵ for their best Permalloy-copper inter-

TABLE II. Determination of the degree of magnetic-coupling from Eqs. (5) and (6).

Specimen	Temperature (K)	ΔH (G)	L (10^{-2} cm)	Γ' (cm/s)	t
Permalloy-K (strong coupling)	5.9	37	1.68	4.7	0.22
Permalloy-K (moderate coupling)	1.1	15	1.97	2.0	0.11
Fe-Li (five samples)	1.1	(Slope from Fig. 9)		5.3	0.14
Permalloy-Cu (strong coupling) (data of Silsbee, Janossy, and Monod)	20–30	268	0.70	20	0.34

face. In this case, the measurement was carried out in the (20–30)-K temperature range and appears to indicate a somewhat stronger coupling than obtained in our alkali-metal specimens. It should be emphasized that all of these numbers are rather crude estimates, since several approximations and assumptions were used in their derivation. The numbers are more likely to be upper limits on Γ' and t , as we have neglected any interfacial relaxation that would contribute to a portion of the CESR linewidth broadening.

The temperature dependencies of the CESR intensity and linewidth displayed in Figs. 3, 4, 7, and 8 are quite remarkable. The linewidth behavior is opposite to that normally encountered in most materials. The only apparent way to include this temperature dependence in the theoretical model of Silsbee, Janossy, and Monod⁵ is to make Γ' a function of the temperature. There is, however, no clear reason why Γ' (or the transmission coefficient t) should depend on the temperature.

To look for the origins of this temperature dependence, it is useful to consider the various parameters, which characterize the potassium or lithium used in this study. In Table I we have listed typical values of several parameters, either measured or calculated at 1.1 K. Some of the numbers were obtained from CESR and electrical conductivity measurements carried out on relatively thick films of each metal prepared by evaporation in the UHV chamber. In our computation of the quantities in Table I, we have used effective-mass ratios for the conduction electrons obtained from de Haas–van Alphen measurements of potassium and from electronic-specific-heat measurements of lithium. The spin depth is given by $\delta_s = [(2/3)v_F\Lambda T_2]^{1/2}$, where Λ is the electronic mean free path. The alkali-metal thickness L in a typical bilayer sample is about 1×10^{-2} cm. Thus, at our lowest temperature the alkali metal is thin compared to δ_s in both potassium and lithium. For lithium, $\Lambda \ll L$, and electron transport in the alkali-metal takes place by diffusion. For potassium, $\Lambda > L$, and electron transport in the alkali metal is mostly ballistic. In the thin ferromagnetic film, electron transport is most likely ballistic in iron and diffusive in Permalloy. As the temperature is raised, thermal phonons reduce the electron mean free path relatively quickly, and electron transport in potassium becomes diffusive by a temperature of a few kelvins. In pure potassium, thermal phonons also contribute to increased spin scattering, and the CESR linewidth broadens. In lithium, thermal phonons make a negligible contribution to the spin-scattering rate. Thus, with increased temperature, δ_s will decrease in both metals, albeit more quickly in potassium, where both Λ and T_2 are reduced by phonon scattering.

One might at first be tempted to argue that the decrease in linewidth at elevated temperature is caused by a reduction in

the mean free path or spin depth. Perhaps the transition from ballistic to diffusive transport in the alkali metal or the transition from $\delta_s \gg L$ to $\delta_s < L$ results in reduced contact between the conduction electrons in the alkali metal and the ferromagnetic film. A careful consideration, however, indicates that this is probably not the case. For $\delta_s \gg L$, the conduction electrons are able to travel several times back and forth across the sample in a spin lifetime. Therefore, the transverse magnetization induced in these electrons at or near resonance is distributed uniformly throughout the volume of the sample. The fraction of the time that a given electron will be found within the ferromagnetic layer, or the rate at which a given electron encounters the interface between the two metals, is not a function of the mean free path but depends only on the relative thicknesses of the two layers. Independent of whether the transport across the sample is ballistic or diffusive, the electron flux encountering the interface will be the same. An analogy is the motion of molecules in an ideal gas. The pressure exerted on the surface of the container by the gas inside is given by the ideal-gas law $PV = nRT$ and is proportional to the molecular flux striking the surface. The flux and pressure remain the same whether the container is thin compared to the mean free path (ballistic trajectories) or thick compared to the mean free path (diffusive motion of the molecules). Likewise, in our samples a transition from $\Lambda \gg L$ to $\Lambda \ll L$ should not effect the total electron flux at the interface nor the rate at which the individual electrons encounter the ferromagnetic film.¹⁵ At still higher temperatures, when $\delta_s < L$ for our bilayer samples, only those electrons within about one spin depth of the ferromagnetic layer can repetitively encounter the interface during the spin lifetime and thus respond strongly under resonant conditions; however, the electron flux at the interface must still be the same as at lower temperature. Therefore, the individual electrons within one spin depth of the interface must continue to interact with the ferromagnetic metal at the same rate experienced at lower temperatures when $\delta_s \gg L$. From these arguments it would appear that the degree of contact between the ferromagnetic film and the resonant electrons in the alkali metal is not a function of temperature, mean free path, or spin depth.

In an effort to see if the low-temperature linewidth broadening is correlated with any other physical parameters of the alkali metal, we have also measured the temperature dependence of the electrical resistivity of one of the metals. We selected lithium, since T_2 is temperature independent and Λ and δ_s depend only on the collision time τ . A lithium layer 1.4×10^{-2} cm in thickness (comparable to that of a typical bilayer specimen) was evaporated onto a glass substrate in the same manner normally used for the fabrication of a bilayer. This thickness was much larger than the residual mean free path, so that electrical resistivity values would be those

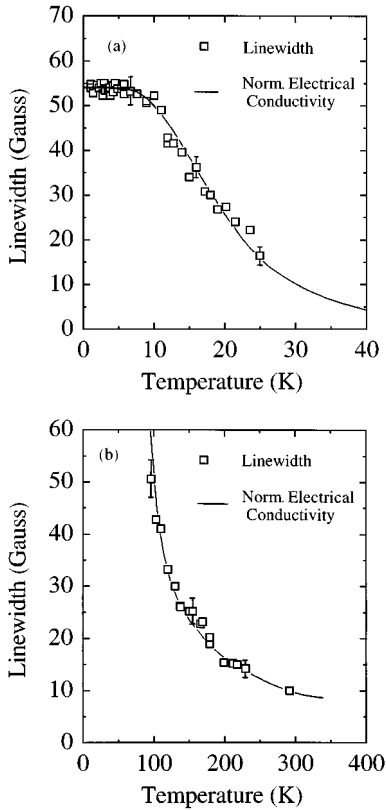


FIG. 11. Comparison of the temperature dependencies of the CESR linewidth in Fe-Li bilayers and the electrical conductivity of bulk lithium. The thicknesses of the bilayer specimens are (a) $L=6.1 \times 10^{-3}$ cm and (b) $L=1.2 \times 10^{-3}$ cm.

of bulk material. The resistivity was measured with the van der Pauw technique¹⁶ using four electrical contacts to the specimen, keeping the total power dissipation $<10^{-7}$ W and making corrections for thermal emf's. The residual resistivity ratio $R(295 \text{ K})/R(1.1 \text{ K})$ was 700. In Fig. 11 we compare the temperature dependencies of the electrical resistivity of bulk lithium and the CESR linewidth of two Fe-Li specimens. In Fig. 11(a) a bilayer thickness of 6.1×10^{-3} cm was chosen so that the CESR temperature dependence could be accurately measured at lower temperatures; in Fig. 11(b) a thickness of 1.2×10^{-3} cm allows one to monitor the temperature dependence in a higher-temperature regime. In the figure, we have plotted the electrical conductivity of the lithium, i.e., the reciprocal of the resistivity, normalized to the CESR linewidth at temperatures of 4.2 K and 200 K for parts (a) and (b), respectively. As can be seen, the linewidth and conductivity plots overlap each other almost exactly. For the thicker sample, both quantities become temperature independent below 6 K and decrease at the same rate for higher temperatures; for the thinner sample, both quantities have about the same temperature dependence between 100 K and room temperature. This implies that the temperature-dependent part of the CESR linewidth of the alkali metal is directly proportional to the electronic scattering time τ of that metal. It should be noted from the numbers in Table I and the fact that the spin depth in lithium is proportional to the square root of the electrical conductivity, that δ_s is always significantly larger than L over the full temperature range shown for the

two samples in Fig. 11. Consequently, the temperature dependence of the linewidth cannot be attributed to a change of regime from $L \ll \delta_s$ to $L > \delta_s$.

It is worthwhile looking at other resonant systems whose linewidths have displayed the same temperature characteristics as we have observed in the CESR to see if there may be some correlation between our system and one of these others. One such system is that of local magnetic moments in a metallic host, an example of which is the dilute copper-chromium alloys studied by Monod and Schultz¹⁷ using transmission electron spin resonance. In such a system, with sufficiently strong coupling between the local moment and the conduction electrons of the metallic host, a single resonant line results whose characteristics depend primarily on $\chi_r = \chi_d/\chi_s$, i.e., the ratio of the impurity static susceptibility to that of the conduction-electron susceptibility. Although χ_s is temperature independent, χ_d generally follows a Curie-Weiss law, giving the same temperature dependence to χ_r . Whenever $\chi_r \ll 1$, the properties of the conduction electron system will dominate the resonance signal; however, when $\chi_r > 1$, as may happen at low temperatures, the intrinsic properties of the local moments will dominate the resonance. In the Cu-Cr alloys a clear narrowing of the linewidth occurs as the temperature is increased from 1 to 25 K. This occurs as χ_r becomes smaller, and the contribution of $1/T_{dl}$ to the linewidth decreases. $1/T_{dl}$ is the spin relaxation rate of the localized moments directly to the lattice.

Is it possible that at the interfaces of our samples some of the Ni and/or Fe diffuses into the alkali metal, producing localized moments that dominate the observed resonance and its temperature dependence? Neither Fe nor Ni are known to have any significant solubility in solid Li or K.¹⁸ Probably the strongest argument against this possibility is the fact that there is no temperature dependence to the measured g values. When local moments are intentionally introduced, the g value also becomes temperature dependent, varying from that of the pure local moment at low temperature (when $\chi_r \gg 1$) to that of the pure metallic host at higher temperatures (when $\chi_r \ll 1$). In all of our bilayer samples the CESR signals consistently give the g value of the pure metal, and no temperature dependence has ever been detected. Furthermore, the observed temperature dependence of the CESR linewidth follows very closely that of the electrical conductivity and is *not* consistent with a Curie-Weiss law that one would expect for local moments.

In addition to preparing samples with a homogeneous distribution of local moments, one can also implant magnetic ions locally at the surface of a metallic sample. Such implanted specimens were fabricated and studied by Monod *et al.*¹⁹ and Hurdequint²⁰ and were considered theoretically by Walker.²¹ This class of samples also displays a strong temperature dependence to the CESR g value and linewidth, with ΔH initially narrowing upon warming from low temperatures. This comes about once again primarily because of a Curie-Weiss-like temperature dependence to the susceptibility of the implanted ions. Although this type of sample is closer to what we would expect to find in our own samples if the Fe or Ni are diffusing into the alkali metal, the line-narrowing process can again be dismissed with the same arguments used for a homogeneous distribution of local moments.

Another case in which a similar temperature dependence for a CESR linewidth has been observed was reported by Magno and Pifer.²² They studied the CESR of metallic bilayers such as Li-Cu and Li-Mn over the temperature range 50–300 K. Their data (Figs. 5–8) display a monotonic decrease in ΔH with higher temperature, with a total variation up to a factor of 5 over the indicated temperature range. A theoretical analysis is carried out in which Maxwell's equations plus a diffusion-modified Bloch equation are solved simultaneously for each metal, utilizing suitable boundary conditions at the common interface and outside surfaces of the sample. In order to fit the data to the theory, they conclude that the transmission coefficient for an electron to cross the interface without spin scattering is very small and that the temperature dependence of the CESR linewidth is caused by the temperature dependence of the coefficient ϵ , which gives the probability of reflection at the interface with spin relaxation. They do not present any mechanisms that would contribute to the temperature dependence of ϵ . However, they do display a very interesting result in the top trace of Fig. 10 in their paper. This is a theoretical calculation of the temperature dependence of ΔH in which all the reflection and transmission coefficients at the interface are held constant. Nevertheless, the linewidth decreases considerably at higher temperatures, much as we see in our samples. The curve is a result of numerical computations, and it is not possible to see analytically within the article what the narrowing mechanism is.

Analytical calculations by Hurdequint²⁰ for the CESR-transmission signal in bilayer samples, under conditions of strong coupling and both layers thin compared to δ_s , predict a single resonance line whose g value and linewidth are weighted averages of the values in the two individual metals, with the weighting factor being the product of the Pauli susceptibility and the thickness of each individual layer. Under these conditions one would expect a Cu-Li specimen to display a monotonically increasing linewidth with higher temperature because of the increased spin-relaxation rate of the copper. This prediction is not in agreement with the experimental data of Magno and Pifer²² nor some of their theoretical plots, such as the one mentioned in their Fig. 10. CESR in bilayer samples was also studied by Vier, Tolleth, and Schultz²³ in their determination of the Pauli spin susceptibility of Li, Cu, and Ag. Their theoretical treatment gives essentially the same results for the g value and linewidth as obtained by Hurdequint. Their experimental measurements are carried out at the three temperatures 5, 10, and 15 K; however, they do not indicate what the temperature dependence of the linewidths was over this limited range. Thus, it is not clear if others have seen the same temperature dependence of CESR linewidths in bilayer samples as reported by Magno and Pifer.²² It is also not clear what physical mechanism produces the temperature dependence displayed in Fig. 10 of their paper.

Yet another system that can exhibit linewidth narrowing with increasing temperature is a pure metal having g anisotropy on the Fermi surface. In this case, the introduction of thermal phonons at higher temperature will scatter the electrons more rapidly between regions of the Fermi surface having different g values, resulting in motional narrowing of the resonance line. Eventually, at high enough temperatures,

phonon-induced spin-lattice relaxation will cause the line to broaden once again as the temperature rises. The frequency and temperature dependence of the CESR signals in both pure aluminum²⁴ and copper^{25,26} appear to indicate the presence of g anisotropy and motional narrowing in these metals. This is especially evident from the higher-frequency measurements. However, the lithium and potassium used in our bilayer samples have never previously given any indication of g anisotropy. The conduction electrons in lithium experience a very weak spin-orbit coupling, and CESR lines as narrow as 30 mG have been observed in highly purified material. Clearly, g anisotropy is negligible in lithium. Potassium, having a highly spherical Fermi surface and CESR linewidths less than 1 G in pure material should also have a negligible g anisotropy. On the other hand, the Fe, which was used in some of the ferromagnetic films, very likely has significant g anisotropy on its Fermi surface. Is it possible that the width of the CESR signal is caused primarily by g anisotropy within the Fe, and that momentum scattering, primarily within the alkali metal, is the mechanism that allows the electrons to experience a different g -value each time they return to the Fe layer? Could this give a mechanism by which the CESR linewidth might follow the temperature dependence of the electrical conductivity of the alkali metal? If this were the case, one might again expect a temperature dependence to the observed g value. Both Cu and Al have temperature-dependent g values, which can be interpreted in terms of a model by Fredkin and Freedman,^{27,28} which contains both g anisotropy and an exchange coupling between the conduction electrons themselves. This temperature dependence is stronger at higher frequencies. We, however, see no temperature dependence in either our reflection measurements at 12 GHz or in our transmission measurements on trilayer specimens at 80 GHz.¹³ Furthermore, from our earlier discussion, we do *not* expect the rate of return of the conduction electrons from the alkali metal back into the ferromagnetic metal to depend upon Λ or δ_s . Thus, this mechanism does not appear to provide the observed temperature dependence or to be the source of the low-temperature line broadening.

A final possibility that we have considered is the spin scattering of conduction electrons within the ferromagnetic film by thermally excited magnons (spin waves). This electron-magnon scattering has been considered by Turov,²⁹ and it can make a significant contribution to the FMR linewidth in metallic ferromagnets. The most likely process is one which is associated with the simultaneous spin flip and momentum scattering of a conduction electron along with the creation or absorption of a magnon. This process has a total change of spin angular momentum of $\Delta S=0$. Its temperature dependence is proportional to $T^{1/2}$ and, therefore, cannot explain our data. Another, less likely scattering event has $\Delta S=\pm\hbar$ and a temperature dependence proportional to $T^{-1/2}$. This involves the momentum scattering of the conduction electron and the creation or absorption of a magnon. However, the spin of the conduction electron is unchanged in the event, and, therefore, this mechanism cannot contribute to the CESR linewidth. Other higher-order processes will have other temperature dependencies, but it seems unlikely

that they can dominate the first-order process, which has the wrong temperature dependence. Thus, this mechanism also appears to be ruled out.

In summary, from the various resonant systems we have considered, we cannot identify one that clearly provides the physical mechanism for the temperature dependence of the linewidth in our specimens. Three systems (the bilayers of Magno and Pifer,²² those with g anisotropy, and those with ferromagnetic magnon scattering) do not produce a large enhancement of the resonance intensity at low temperature such as the one we observe. The temperature dependence of our data thus remains unexplained. A theoretical attempt to understand the source of this temperature dependence would be welcomed.

V. CONCLUSION

Fabrication techniques have been developed and reported that allow one to make magnetically coupled metallic bilayer samples consisting of a ferromagnetic metal and an alkali metal. A study of the interaction between the FMR of the

ferromagnetic metal and the CESR of the alkali metal provides a probe for measuring the degree of magnetic coupling between the two metals. A novel feature of the data reported here is the narrowing of the CESR line with increasing temperature. Further theoretical efforts are needed to understand the temperature dependence of the CESR linewidth and intensity in the low-temperature regime.

ACKNOWLEDGMENTS

This research was supported in part by National Science Foundation Grant Nos. DMR-9120274 and DMR-9400553 and the generosity of Vacuum/Atmospheres Company, Hawthorne, CA. The authors would like to thank Dr. A. Wijeratne, University of Sri Jayawardenapura, Sri Lanka, for his assistance in the initial design of the sample-preparation chamber and F. Fey and Dankun Yang for their assistance with the data analysis. Helpful conversations with J. J. Chang, H. Hurdequint, M. B. Johnson, R. Magno, S. Schultz, and M. B. Walker are also gratefully acknowledged.

-
- ¹A. Janossy, Phys. Rev. B **21**, 3793 (1980).
²A. Janossy and P. Monod, Solid State Commun. **18**, 203 (1976).
³A. Janossy and P. Monod, Phys. Rev. Lett. **37**, 612 (1976).
⁴*Amorphous Magnetism*, edited by H. O. Hooper and A. M. de Graaf (Plenum, New York, 1973).
⁵R. H. Silsbee, A. Janossy, and P. Monod, Phys. Rev. B **19**, 4382 (1979).
⁶A. T. Wijeratne and G. L. Dunifer, Phys. Rev. B **41**, 5017 (1990).
⁷D. S. Montgomery and M. B. Walker, Phys. Rev. B **19**, 1566 (1979).
⁸Another model, proposed by Overhauser, consists of a charge-density-wave ground state for potassium. See, for example, A. W. Overhauser, Adv. Phys. **27**, 343 (1978).
⁹D. A. H. Mace, G. L. Dunifer, and J. R. Sambles, J. Phys. F **14**, 2105 (1984).
¹⁰A. Roth, *Vacuum Technology* (North-Holland, New York, 1976).
¹¹G. L. Dunifer, J. R. Sambles, D. A. H. Mace, and A. T. Wijeratne, J. Phys. F **17**, 1581 (1987).
¹²C. Kittel, Phys. Rev. **71**, 270 (1947).
¹³J. S. Payson, D. Yang, and G. L. Dunifer (unpublished).
¹⁴M. R. Menard and M. B. Walker, Can. J. Phys. **52**, 61 (1974).
¹⁵Argument due to M. B. Walker (private communication).
¹⁶L. J. van der Pauw, Philips Res. Rep. **13**, 1 (1958).
¹⁷P. Monod and S. Schultz, Phys. Rev. **173**, 645 (1968).
¹⁸W. G. Moffatt, *The Handbook of Binary Phase Diagrams* (Genum, Schenectady, NY, 1984).
¹⁹P. Monod, H. Hurdequint, A. Janossy, J. Obert, and J. Chaumont, Phys. Rev. Lett. **29**, 1327 (1972).
²⁰H. Hurdequint, thesis, docteur 3^{ème} cycle, Université de Paris-Sud, Centre d'Orsay, 1973.
²¹M. B. Walker, Phys. Rev. Lett. **30**, 891 (1973).
²²R. Magno and J. H. Pifer, Phys. Rev. B **10**, 3727 (1974).
²³D. C. Vier, D. W. Tolleth, and S. Schultz, Phys. Rev. B **29**, 88 (1984).
²⁴G. L. Dunifer and M. R. Pattison, Phys. Rev. B **14**, 945 (1976).
²⁵D. Lubzens and S. Schultz, Phys. Rev. Lett. **36**, 1104 (1976).
²⁶T. M. Hsu, M. R. Pattison, and G. L. Dunifer (unpublished).
²⁷D. R. Fredkin and R. Freedman, Phys. Rev. Lett. **29**, 1390 (1972).
²⁸R. Freedman and D. R. Fredkin, Phys. Rev. B **11**, 4847 (1975).
²⁹E. A. Turov, in *Ferromagnetic Resonance*, edited by S. V. Vonsovskii (Pergamon, Oxford, 1966), Chap. V.
³⁰A. A. Abd El-Rahman, M. Elliott, and W. R. Datars, J. Phys. F **15**, 859 (1985).
³¹J. D. Filby and D. L. Martin, Proc. R. Soc. London Ser. A **276**, 187 (1963).